Self-Movement Inducing On-Demand Pattern of Mesoporous Silica Thin Film with Oriented Mesochannels

ARTICLE *in* CHEMISTRY OF MATERIALS · OCTOBER 2009

Impact Factor: 8.35 · DOI: 10.1021/cm9022985

6 AUTHORS, INCLUDING:

Xuemin Lu
Shanghai Jiao Tong University
56 PUBLICATIONS **451** CITATIONS
SEE PROFILE

Qinghua Lu
Shanghai Jiao Tong University
128 PUBLICATIONS **2,682** CITATIONS
SEE PROFILE

DOI:10.1021/cm9022985

CHEMISTRY OF MATERIALS
Article

Self-Movement Inducing On-Demand Pattern of Mesoporous Silica Thin Film with Oriented Mesochannels

Bin Su, Xuemin Lu, Qinghua Lu,* Xin Li, Changquan You, and Jia Jia

School of Chemistry and Chemical Engineering and the State Key Laboratory of Metal Matrix Composites, Shanghai Jiao Tong University, Dongchuan Road, No. 800, Shanghai, 200240, P. R. China

Received July 27, 2009. Revised Manuscript Received September 18, 2009

An on-demand pattern of mesoporous thin film with oriented mesochannels was attractive for the application of mesoporous thin film in wide fields. In this work, we reported the preparation of such a featured mesoporous silica thin film based on self-movement of solution on a laser pattern-irradiated polyimide film. SEM and EDS observation confirmed that the deposition of silica sol precursor showed strict selectivity on such an irradiated polyimide film surface with aid of photomask: aggregation occurred only on the irradiated region and not on the nonirradiation region. TEM and In-plane XRD results proved that mesochannels in the patterned silica thin film oriented along laser induced surface periodic microgrooves (LIPS). The selective pattern of silica sol solution on the laser pattern-irradiated polyimide surface was attributed to the difference in surface energy between irradiated and nonirradiated regions according to the calculating result based on the contacting angle measurement, which leads to self-movement of silica solution from the low surface energy to high surface energy. The alignment of mesochannels in the patterned silica film resulted form the confining effect of surface microgrooves. Such a selectivity deposition provides a powerful tool to control the on-demand pattern of mesoporous silica film with oriented mesochannels. Further experiments proved that the on-demand control of pattern is applicable not only for the pure silica mesoporous system, but also for other hybrid systems based on mesoporous materials.

Mesoporous materials, formed by the organization of inorganic precursors around a surfactant mesophase template, have attracted great attention since the first successful synthesis of nanoporous particles.[1,2] Because of their high surface areas, large specific pore volumes, and narrow distributions of pore diameter, this feature materials have been utilized in catalyst support,[3] adsorbent and separation,[4] controlled release[5] and other extending applications. Among a series of different forms such as powder, fiber, bulk, and film, interest in thin films of these materials has grown considerably recently for applications such as chemical/gas sensors,[6,7] specific optical materials,[8,9] and biochemical analysis.[10]

Precisely patterning of mesoporous or mesostructured thin films (MTF, in brief) on substrate are very important in the view of both the scientific and technical points.[11−13] Although patterned MTFs have been developed through micromolding in capillaries (MIMIC),[8,14−17] ultraviolet (UV) irradiation,[18−21] X-ray direct writing,[22] electron-beam lithography (EBL),[23] low-energy electron-beam

*Corresponding author. E-mail: qhlu@sjtu.edu.cn.

(1) Yanagisawa, T.; Shimizu, T.; Kuroda, K.; Kato, C. *Bull. Chem. Soc. Jpn.* **1990**, *63*, 988.
(2) Kresge, C. T.; Leonowicz, M. E.; Roth, W. J.; Vartuli, J. C.; Beck, J. S. *Nature* **1992**, *359*, 710–712.
(3) Cortial, G.; Siutkowski, M.; Goettmann, F.; Moores, A.; Boissière, C.; Grosso, D.; Floch, P. L.; Sanchez, C. *Small* **2006**, *2*, 1042.
(4) Baskaran, S.; Liu, J.; Domansky, K.; Kohler, N.; Li, X. H.; Coyle, C.; Fryxell, G. E.; Thevuthasan, S.; Williford, R. E. *Adv. Mater.* **2000**, *12*, 291.
(5) De, M.; Ghosh, P. S.; Rotello, V. M. *Adv. Mater.* **2008**, *20*, 4225.
(6) Yamada, T.; Zhou, H. S.; Uchida, H.; Tomita, M.; Ueno, Y.; Ichino, T.; Honma, I.; Asai, K.; Katsube, T. *Adv. Mater.* **2002**, *14*, 812.
(7) Qi, Z. M.; Honma, I.; Zhou, H. S. *Appl. Phys. Lett.* **2006**, *88*, 053503.
(8) Goettmann, F.; Moores, A.; Boissière, C.; Floch, P. Le.; Sanchez, C. *Small* **2005**, *1*, 636.
(9) Sanchez, C.; Boissière, C.; Grosso, D.; Laberty, C.; Nicole, L. *Chem. Mater.* **2008**, *20*, 682.
(10) Buranda, T.; Huang, J. N.; Ramarao, G. V.; Ista, L. K.; Larson, R. S.; Ward, T. L.; Sklar, L. A.; Lopez, G. P. *Langmuir* **2003**, *19*, 1654.
(11) Moller, K.; Bein, T. *Chem. Mater.* **1998**, *10*, 2950.
(12) Hartmann, M. *Chem. Mater.* **2005**, *17*, 4577.
(13) Ariga, K.; Vinu, A.; Hill, J. P.; Mori, T. *Coord. Chem. Rev.* **2007**, *251*, 2562.
(14) Yang, P. D.; Wirnsberger, G.; Huang, H. C.; Cordero, S. R.; McGehee, M. D.; Scott, B. J.; Deng, T.; Whitesides, G. M.; Chmelka, B. F.; Buratto, S. K.; Stucky, G. D. *Science* **2000**, *287*, 465.
(15) Trau, M.; Yao, N.; Kim, E.; Xia, Y.; Whitesides, G. M.; Aksay, I. A. *Nature.* **1997**, *390*, 674.
(16) Scott, B. J.; Wirnsberger, G.; Stucky, G. D. *Chem. Mater.* **2001**, *12*, 3140.
(17) Wirnsberger, G.; Yang, P. D.; Huang, H. C.; Scott, B.; Deng, T.; Whitesides, G. M.; Chmelka, B. F.; Stucky, G. D. *J. Phys. Chem. B* **2001**, *105*, 6307.
(18) Hozumi, A.; Sugimura, H.; Hiraku, K.; Kameyama, T.; Takai, O. *Adv. Mater.* **2001**, *13*, 667.
(19) Dattelbaum, A. M.; Amweg, M. L.; Ecke, L. E.; Yee, C. K.; Shreve, A. P.; Parikh, A. N. *Nano. Lett.* **2003**, *3*, 719.
(20) Clark, T., Jr.; Ruiz, J. D.; Fan, H.; Brinker, C. J.; Swanson, B. I.; Parikh, A. N. *Chem. Mater.* **2000**, *12*, 3879.
(21) Wang, J.; Stucky, G. D. *Adv. Mater.* **2004**, *14*, 409.
(22) Cagnol, F.; Grosso, D.; Soler-Illia, G. J.; Crepaldi, E. L.; Babonneau, F.; Amenitsch, H.; Sanchez, C. *J. Mater. Chem.* **2003**, *13*, 61.
(23) Wu, C.-W.; Aoki, T.; Kuwabara, M. *Nanotechnology* **2004**, *15*, 1886.

Published on Web 10/05/2009

(LEEB) irradiation,[24] inkjet printing,[25] dip-pen lithography,[26−29] site-selective deposition[30−32] and pattern-transfer method,[33] MTF-based devices have not met with breakthroughs. A major hurdle preventing their practical applications is the disordered arrangement of mesochannels inside the patterned regions. Ordered porous architectures (e.g., uniaxially orientated) are usually more efficient than disordered pore structures due to optimized pathway through the oriented pores leading to enhanced transport of guest species.[34] Actually, to realize more practicable MTFs based devices, the on-demand pattern of mesoporous film with oriented mesochannels needs to be done.[35,36] Some approaches have been provided to prepare full oriented mesochannels on substrates such as mica,[37] oriented silicon wafers,[38] rubbed polyimide,[39−41] Langmuir film,[42] photo-oriented polymer film,[43−46] or with aid of out force fields such as magnetic,[47] hot jet air flow.[48] However, little attention has been paid so far to precise patterning of MTFs with controlled oriented mesochannels.

In this article, we report the on-demand deposition of mesoporous silica thin film with oriented mesochannels on a polymer film surface as supporting substrate. The deposition procedure, as shown in Scheme 1, was based on self-movement of silica sol solution because of the patterned distribution of surface energy on this substrate. To obtain such a substrate, a beam of nanosecond pulsed laser was employed to irradiate a polyimide (PI) film with aid of photomask or by direct writing.

Scheme 1. Fabrication Process for Patterned Silica Thin Film with Uniaxial Orientation of Mesochannels[a]

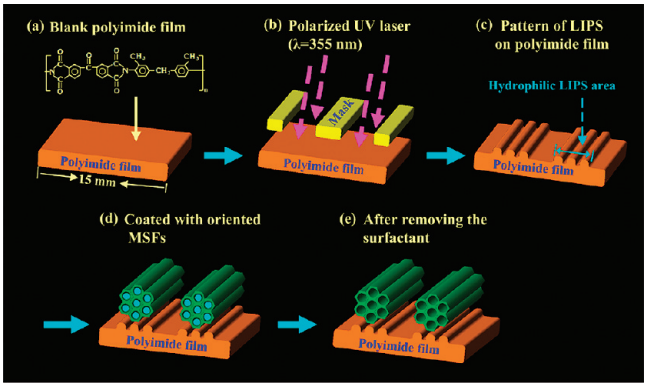

[a] (a) Chemical structure of PI; (b) polarized laser irradiation on PI substrate through a photomask; (c) patterned region of PI surface after laser irradiation; (d) on-demand deposition of silica sol solutions on PI substrate; (e) patterned silica MTF after removal of organic surfactant.

The laser-irradiation-induced change of surface energy was calculated by measuring the surface contact angle of water. The pattern of the surface with different surface energy drove the self-movement of silica sol solution deposited atop of it from low surface energy to high surface energy. SEM and EDS spectrum confirmed that precise on-demand pattern of mesoporous silica film was formed on the laser pattern-irradiated polymer film. Simultaneously, TEM and in-plane XRD measurement confirmed that the mesochannels in the thin film was also controlled to be aligned in a desired direction because of the confining effect of surface microgrooves. Finally, as a proof of the results presented in this article, we successfully carried out the selective deposition of quantum-dot/silica hybrid film, which shows great potential in designing a new kind of nanoadvanced photoelectronic device.

Experimental Section

PI film[49] was prepared by the dissolution of PI in chloroform (10 wt %) and spin-coated on clean glass, silicon, or aluminum wafers for different experimental measurements. After being baked at 100 °C for 2 h, the thickness of the PI film was about 1 μm according to ellipsometry. The PI film was irradiated by a beam of nanosecond pulsed laser. Detailed procedure on the preparation and AFM image of LIPS was presented in Supporting Information. (see the Supporting Information, Figure S1)

Mesostructured thin film was prepared on PI film using dip-coating method through evaporation-induced self-assembly (EISA) procedure.[50] A mixture of Pluronic 123 (P123), hydrochloric acid (HCl), deionized water, ethanol and tetraetoxysilane (TEOS) was stirred for 3 h at 60 °C. The reactant molar ratio of TEOS/P123/H_2O/HCl/C_2H_5OH was 1/0.01/6.5/0.01/15−35. The irradiated PI-coated substrate was immersed vertically in the sol solution for 10 s at room temperature then lifted up at a speed of 0.1−2 mm/s with a relative humidity of about 40−50%. After lifting up, the substrate was blown dry with N_2 gas. The organic surfactant in the mesoporous thin film was

(24) Hozumi, A.; Kimura, T. *Langmuir* **2008**, *24*, 11141.
(25) Fan, H.; Lu, Y.; Stump, A.; Reed, S.; Baer, T.; Schunk, R.; Perez-Luna, V.; Lopez, G. P.; Brinker, C. J. *Nature* **2000**, *405*, 56.
(26) Piner, R.; Zhu, J.; Xu, F.; Hong, S.; Mirkin, C. A. *Science* **1999**, *283*, 661.
(27) Fan, H.; Reed, S.; Baer, T.; Schunk, R.; López, P.; Brinker, C. J. *Microporous Mesoporous Mater.* **2001**, *44*−*45*, 625.
(28) Salaita, K.; Wang, Y.; Mirkin, C. A. *Nat. Nanotechnol.* **2007**, *2*, 145.
(29) Su, M.; Liu, X.; Li, S.-Y.; Dravid, V. P.; Mirkin, C. A. *J. Am. Chem. Soc.* **2002**, *124*, 1560.
(30) Tender, L. M.; Worley, R. L.; Fan, H.; Lopez, G. P. *Langmuir* **1999**, *12*, 5515.
(31) Yang, H.; Coombs, N.; Ozin, G. A. *Adv. Mater.* **1997**, *9*, 811.
(32) Hozumi, A.; Kojima, S.; Nagano, S.; Seki, T.; Shirahata, N.; Kameyama, T. *Langmuir* **2007**, *23*, 3265.
(33) Hozumi, A.; Kizuki, T.; Inagaki, M.; Shirahata, N. *J.Vac.Sci. Technol.A.* **2006**, *24*, 1494.
(34) Walcarius, A.; Kuhn, A. *Trac-Trend Anal. Chem.* **2008**, *27*, 593.
(35) Brinker, C. J.; Dunphy, D. R. *Curr. Opin. Colloid. Interface Sci.* **2006**, *11*, 126.
(36) Innocenzi, P.; Malfatti, L.; Kidchob, T.; Falcaro, P. *Chem. Mater.* **2009**, *21*, 2555.
(37) Suzuki, T.; Kanno, Y.; Morioka, Y.; Kuroda, K. *Chem. Commun.* **2008**, 3284.
(38) Miyata, H.; Kuroda, K. *J. Am. Chem. Soc.* **1999**, *121*, 7618.
(39) Miyata, H.; Kuroda, K. *Chem. Mater.* **2000**, *12*, 49.
(40) Miyata, H.; Kuroda, K. *Chem. Mater.* **2002**, *14*, 766.
(41) Suzuki, T.; Miyata, H.; Watanabe, M.; Kuroda, K. *Chem. Mater.* **2006**, *18*, 4888.
(42) Miyata, H.; Kuroda, K. *Adv. Mater.* **1999**, *11*, 1448.
(43) Hara, M.; Nagano, S.; Kawatsuki, N.; Seki, T. *J. Mater. Chem.* **2008**, *18*, 3259.
(44) Fukumoto, H.; Nagano, S.; Kawatsuki, N.; Seki, T. *Chem. Mater.* **2006**, *18*, 1226.
(45) Fukumoto, H.; Nagano, S.; Kawatsuki, N.; Seki, T. *Adv. Mater.* **2005**, *17*, 1035.
(46) Kawashima, Y.; Nakagawa, M.; Ichimura, K.; Seki, T. *J. Mater. Chem.* **2004**, *14*, 328.
(47) Yamauchi, Y.; Sawada, M.; Sugiyama, A.; Osaka, T.; Sakka, Y.; Kuroda, K. *J. Mater. Chem.* **2006**, *16*, 3693.
(48) Su, B.; Lu, X. M.; Lu, Q. H. *J. Am. Chem. Soc.* **2008**, *130*, 14356.
(49) Lu, Q. H.; Yin, J.; Xu, H. J.; Zhang, J. M.; Sun, L. M.; Zhu, Z. K.; Wang, Z. G. *J. Appl. Polym. Sci.* **1999**, *72*, 1299.
(50) Lu, Y. F.; Ganguli, R.; Drewien, C. A.; Anderson, M. T.; Brinker, C. J.; Gong, W.; Guo, Y. X.; Soyez, H.; Dunn, B.; Huang, M. H.; Zink, J. I. *Nature* **1997**, *389*, 364.

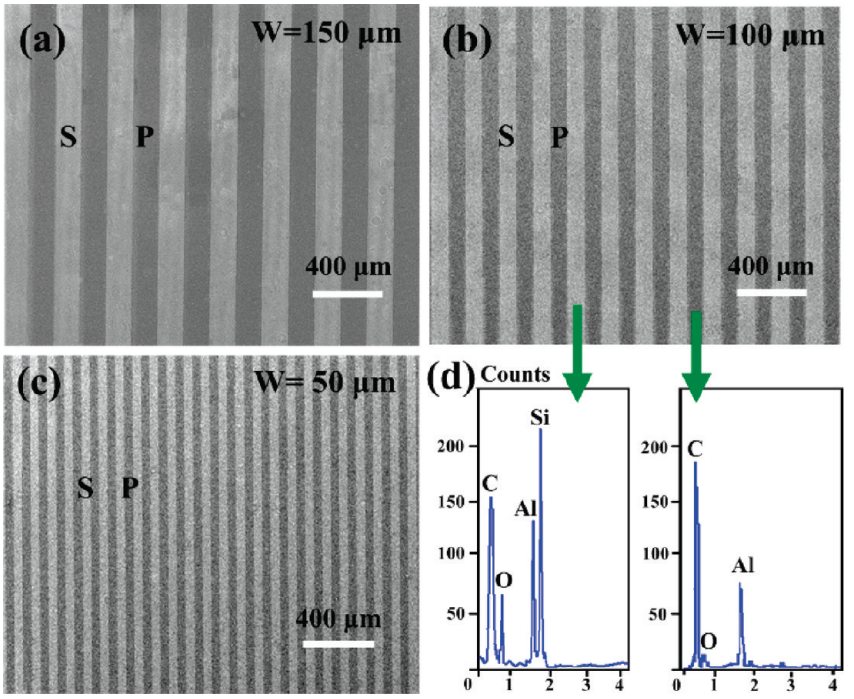

Figure 1. (a−c) SEM images of site-selective aggregation of silica MTFs on laser-irradiated PI substrate with different periods; (d) EDS spectrum of patterned silica MTFs at different regions. Dip rate is 0.1 mm/s and the room humidity is 50%. W, S, and P are represented as the width of linear region, silica thin film, and blank PI regions, respectively.

removed using ethanol extraction method for 48 h in 78 °C, which was confirmed by the disappearance of the C−H stretching vibration peak at 2840 - 2970 cm^{-1}. (see the Supporting Information, Figure S2)[51] The thickness of the silica MTFs as determined by ellipsometry was ca.200 nm.

The CdTe incorporated hybrid MTFs was prepared as follows: oil-soluble CdTe quantum dots with particle size of ca. 3 nm (purchased from ZhongDS investment Co. Ltd., China) were mixed with above silica precursor solution directly (v/v = 1/10). The irradiated PI substrate was immersed vertically into this solution for 10 s at room temperature and then lifted at 0.1 mm/s into an atmosphere with a relative humidity of ca. 40−50%. Other post-treatments were the same as above.

The topography of the irradiated PI film was measured by atomic force microscopy (AFM, Digital Instruments Nano Scope IIIa) in contact mode. Field emission scanning electron microscopy with EDS (FE-SEM, JEOL JSM-7401F) was employed to investigate the topography of silica MTFs. In order to avoid the interference from silicon element in glass wafer for EDS observations, the PI substrate was coated on aluminum wafer. The transmission electron micrographs (TEM) were taken on a JEOL TEM-2100 operated at an accelerating voltage of 200 KeV. Powder θ-2θ X-ray diffraction (XRD) patterns were taken on an X-ray Polycrystalline Diffractometer using Cu Kα radiation (D8 ADVANCE, Bruker). In-plane XRD measurement were performed using Cr−Kα radiation (D8 Discover GADDS General Area Detector Diffraction System, Bruker). The orientation degree of mesochannels was calculated according to ref 44.

The sessile drop method was used for the static contact angle measurement by using a contact angle instrument (OCA 20, DataPhysics, Germany). Droplets with typical volumes (3 μL) of ethanol or Milli-Q water were released from the syringe onto the sample surface for measurement.

Results and Discussion

On-Demand Deposition of Silica MTFs on PI Surface. A mesostructured surfactant/silica thin film was prepared by dipping a PI-coated glass substrate into the silica precursor sol solution containing Pluronic 123 as surfactant template and lifting out with a speed of 0.1 mm/s at room temperature. Before used, the PI surface was irradiated by a beam of nanosecond pulsed laser with aid of photomask of a stripe pattern. The period of the stripe pattern ranges from 50 to 100 μm. The humidity of the environment was ca. 50%. Figure 1a−c is the SEM images of patterned as-synthesized silica thin films on the irradiated PI film. As clearly seen in these images, the silica thin film was selective aggregation on the laser irradiated regions of PI surface, whereas the nonirradiated regions of the PI surface remains free of deposition. After ethanol extraction of the surfactant, the selectivity of silica thin film was perfectly remained.

The selective aggregation of silica thin film on the pattern-irradiated PI film was further confirmed by EDS observation (Figure 1d). In order to avoid the interference of silicon element of glass substrate, aluminum was used as supporting wafer in the work. An absorption peak (1.78 eV) ascribed to silicon element appeared in the EDS spectra of irradiated area, while not found in that of nonirradiated area, proving the perfect selective deposition of silica thin film on the pattern-irradiated area. The peak of aluminum element (1.56 eV) is due to the employment of aluminum wafer.

(51) Hua, Z. L.; Shi, J. L.; Wang, L.; Zhang, W. H. *J. Non-Cryst. Solids* **2001**, *292*, 177.

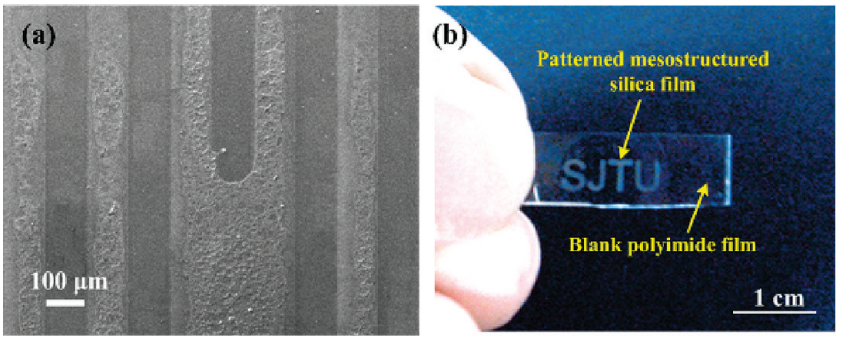

Figure 2. (a) Liquid bridge appeared on as-deposited silica thin film, lifting speed 1 mm/s; (b) optical image of alphabetical patterned silica film with perfectly selectivity, lifting speed 0.1 mm/s.

It was widely accepted that mesoporous materials were formed by the organization of inorganic precursor around a surfactant mesophase template.[50] Previous research also found that film formation was due to the adsorption of organic surfactant molecules or the aggregation of silica particles on the substrate.[52,53] In this work, when the substrate freshly emerged from sol solution, the silica sol solution completely covered on the whole surface of the PI surface: both the irradiated and nonirradiated regions. Subsequently, silica sol solution moved quickly from the nonirradiated regions to irradiated regions. This phenomenon indicated that the selective pattern of silica thin film was resulted not from the selective adsorption of surfactant molecules or silica precursor on the PI surface, but the surface droved self-movement of the silica sol solution deposited atop the polymer surface.

Different factors were investigated to control the pattern of silica thin film on the laser irradiated PI surface. According to previous research on EISA procedure,[52] the formation of silica MTFs was related to many competing factors over a short time scale (generally on the order of seconds), including the evaporation of the solvent, self-assembly of micelles and the inorganic phases. On the other hand, the final pattern of silica MTFs resulted from the self-movement of silica sol solution on polymer surface, so the time scale match between moving in horizontal and vertical directions and solidify of sol solution was a crucial factor in determining the quality of surface pattern. Lifting speed affected the time scale of the movement in both directions. High lifting speed leads to rapid exposure of liquid film to the environment, and then the rapid solidification of film, which reduced the time scale of sol solution in horizontal directions. Wherever, slow lifting direction will be helpful in slowing the solidification, which will provide more times for the movement of silica sol solution. First we investigated the effect of lifting speed on the final formation of pattern of silica thin film. The size of stripe pattern of photomask was fixed to be 100 μm. When the lifting speed was over 1 mm/s, liquid bridge appeared cross the irradiated and nonirradiated regions due to relatively fast solidification of the liquid film as shown in Figure 2a; and when the lifting speed was below 0.5 mm/s, the sol solution was selectively aggregated on the irradiated region of PI film. If we further slow down the lifting speed, the selectivity was perfectly kept even in larger scale of periodicity because remaining enough moving time before the solidification of sol liquid film. As shown in Figure 2b, an irregular pattern with alphabet "SJTU" was used to prove the effectiveness of this approach at millimeter scale. The lifting speed was 0.1 mm/s. Perfect selectivity was kept in such a large size scale. Second, we fixed the lifting speed to be 0.5 mm/s and used photomasks with different periodicities. The film showed strict site-selectivity when the periodicity was in the range of 50−100 μm, whereas the site-selectivity was degraded when the periodicity was greater than 150 μm.

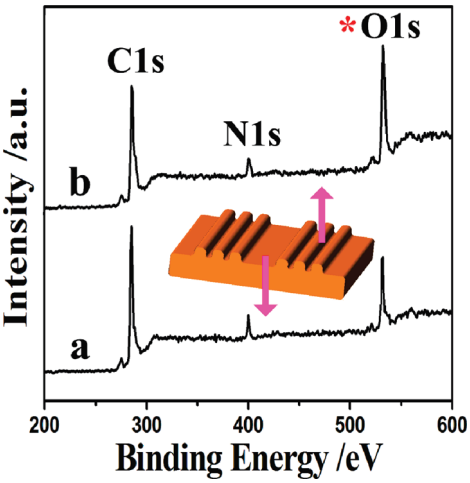

Figure 3. XPS spectrum of (a) nonirradiated and (b) irradiated regions on PI films.

The site-selectivity ascribes to the self-movement of sol solution due to the difference of surface energy of patterned irradiated surface at different regions. To testify this suppose, we measured the change of chemical component of PI surface after laser irradiation by using XPS (Figure 3). It is clearly presented that an oxygen-rich surface was generated in the regions with laser irradiation in comparison with that in blank PI film (see the Supporting Information, Table S1, with Figure S3 of C1s spectra of PI surface before and after irradiation). This change was mainly from the breakage of chemical bonds of

(52) Lee, C. H.; Lu, Y. F.; Shen, A. Q. *Phys. Fluids* **2006**, *18*, 052105.
(53) Brinker, C. J.; Hurd, A. J.; Schunk, P. R.; Frye, G. C.; Ashley, C. S. *J. Non-Cryst. Solids*. **1992**, *147*, 424.

polymer molecules, leading to the occurrence of a large amount of hydrophilic groups (e.g., −COOH, −OH) in the irradiated regions. The enrichment of the polar group on the surface led to the increase in the surface energy in comparison with that of nonirradiated PI film. This change can be confirmed by the decreasing water contact angle on the PI film: the contact angle was about 81° before irradiation and decreased to 36° after irradiation.

On the basis of this information, the effect of surface energy on the pattern formation can be quantitatively estimated. First, we calculated the driving force of the sol solution for moving from low energy area to high energy area on the patterned film surface. To simply this process, water was used as model solution. The driving force for this self-movement lies in the difference of surface energy of the polymer film surface and can be expressed by eq 1.[54,55] The resist force comes from the contact angle hysteresis on surface with low surface energy as eq 2.[54,55] When the driving force is stronger over the resistant force, the self-movement of water droplet on the substrate can occur spontaneously.

$$\text{The driving force}: \delta F = \gamma_{\text{water}}(\cos\theta_{\text{high}} - \cos\theta_{\text{low}}) \quad (1)$$

Where γ_{water} is the surface tension of water. θ_{high} and θ_{low} are the water contact angle on the high-energy area and low-energy area, respectively.

$$\text{The resistant force}: \delta f = \gamma_{\text{water}}(\cos\theta_{\text{r}} - \cos\theta_{\text{a}}) \quad (2)$$

Where θ_{r} and θ_{a} are the receding and the advancing contact angle of water on the low-energy area, respectively. The laser induced change of surface energy can be characterized by using the change of contact angle of water before and after laser irradiation. So the driving force of water on the patterned film surface can be calculated by measuring the contacting angle of water. For fresh PI surface, the receding and advancing contacting angle of water: θ_{r} and θ_{a} are 53 and 83°. The resultant force ($\delta F - \delta f$) is ca.12.99 mN/m (>0), indicating that it is possible for the droplet to move spontaneously from hydrophobic to hydrophilic area. Further, a more direct experiment was conducted to observe the self-movement of liquid on such an irradiated surface. A drop of ethanol was put across irradiated and nonirradiated regions. The drop of ethanol liquid moved from nonirradiated part to irradiated regions in very short time (Figure 4).

The above results proved that a drop in aqueous or alcoholic solution on such a laser irradiated substrate can self-moved from nonirradiated regions to irradiated regions of a planar PI surface. On the other hand, we should consider the effect of gravity of sol solution on the movement in the dip-coating process. When the irradiated substrate was vertically lifted out from the silica sol solution, the silica sol solution covered on blank PI region can be split and self-moved from blank PI region to irradiated regions under the condition of force balance as shown in Figure 5. Final selectivity of sol solution on the laser irradiated PI surface was controlled by the force of $F_{\text{resultant}}$. The $F_{\text{resultant}}$ can be divided into two parts: the horizontal driving force (F_{driving}) caused by the different surface energy in regions with/without irradiation as calculated above, and vertical resultant force of sol's gravity force (G) and frictional force (f) caused by the relative movement between sol solution and PI surface. Therefore, separating sol solutions, which were covered on blank polyimide region, have to move horizontally and vertically, respectively. For the horizontal movement, the

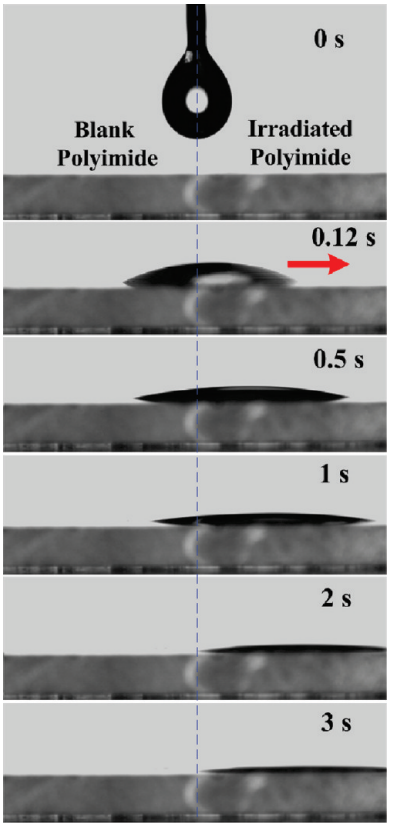

Figure 4. Self-movement of ethanol droplet released onto the borderline of regions without (left) and with (right) laser irradiation. The ethanol droplet quickly moved toward irradiated region on PI substrate.

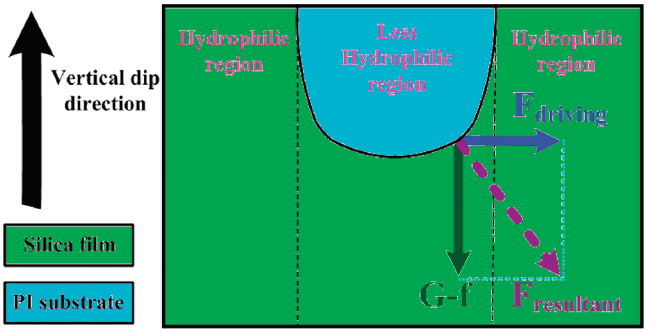

Figure 5. Force balance of sol solution on the linear patterned substrate dipped vertically, F_{driving}, G, f, and $F_{\text{resultant}}$ are represented as the driving force caused by the different interfacial force between high energy area and low energy area, gravitational force of sol solution, frictional force between sol and substrate, and resultant force, respectively.

(54) Lee, W.; Laibinis, P .E. *J. Am. Chem. Soc.* **2000**, *122*, 5395.
(55) Quere, D. *Rep. Prog. Phys.* **2005**, *68*, 2495.

moving time (T_1) was just relative to the distance, i.e., the width of linear regions, when droving force was invariable. For the movement in vertical direction, the moving time of this process (T_2) was mainly affected by the evaporation of solvent and the lifting speed. The quicker lifting speed and the quicker solvent evaporation, the shorter will be the solidification time. Accordingly, perfect patterned thin films can only appear when T_1 was smaller than T_2 because sol solutions have enough time to move to irradiated regions.

According to our previous research, LIPS was formed on the polymer surface when it is irradiated by a laser beam.[56] The existence of LIPS leads to the anisotropy not only in surface topography but also in surface wetting properties.[57] the direction of LIPS also may affect the movement of sol solution deposited atop of it. We further investigated the effect of lifting direction relative to LIPS on the selectivity of sol solution on the patterned silica film area. We lifted the PI-coated glass in two directions: parallel and perpendicular to the LIPS, respectively. No matter what the relationship between lifting direction and surface microgrooves, perfect selectivity of silica sol solution on the laser irradiated PI surface was kept (see the Supporting Information, Figure S4).

Orientation of Mesochannels in the Silica Pattern. Laser irradiation led to the change of PI surface wetting properties, resulting into the pattern formation of silica thin film. These strictly selectivity shows potential in controlling the on-demand pattern of mesoporous thin film. On the other hand, laser irradiation also led to the appearance of surface microgrooves atop of PI film. The direction of surface microgrooves only depended on the polarization of incident laser, which can be adjusted freely according to different requirement. In our previous report, we found that silica mesochannels aligned along the surface microgrooves.[58] This orientation was attributed to the confining effect of surface microgrooves on the micelles formed by organic surfactant molecules, which finally leads to the formation of silica mesochannels. On the pattern-irradiated PI surface, as we pointed out above, the motion of silica sol solution include movement in two directions: horizontal and vertical, which is slightly different form that occurring in the procedure of preparing whole films through EISA. Here, we investigated the microscopic orientation of mesochannels in the selectively deposited silica thin film. Figure 6a is a typical cross-sectional TEM image of the silica MTF sliced perpendicular to the LIPS direction. The mesochannels are aligned parallel to the PI surface and along the laser induced microgrooves. The orientation of the mesochannels is not only limited to those in the trench of the surface microgrooves but also extends to the film above the surface microgrooves. This image proves that the mesochannels were highly oriented over a range of at least several hundred nanometers.

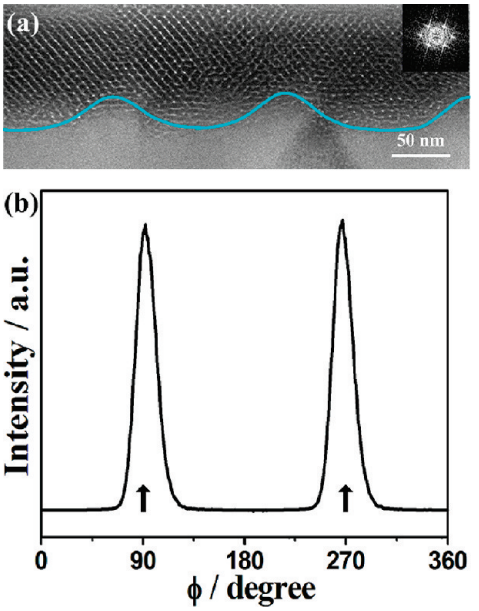

Figure 6. (a) Cross-section TEM image of mesoporous silica film on LIPS surface, the film was sliced across the LIPS section; (b) in-plane XRD profile of mesoporous silica thin film, the arrows indicated the direction of LIPS.

Although the HR-TEM image is a direct and precise method of determining the orientation of mesochannels relative to the substrate, it can only provide orientation information in a very limited area. Φ-scanning in-plane XRD has proved to be a useful tool and has the ability to measure the relative large area. The pattern obtained from in-plane XRD measurements can provide information concerning the lattice plane normal to the film surface and can be used to quantitatively estimate the degree of orientation of the mesochannels in mesoporous silica thin film. Accordingly, in-plane XRD observation was employed to detect the orientation of mesochannels in silica thin film on LIPS surface. The LIPS direction was set to be perpendicular to the incident X-rays at $\Phi = 0°$. Figure 6b presents the profile of in-plane XRD of mesoporous silica thin film on pattern irradiated PI film. Two peaks are observed at the position of 90 and 270°, with narrow directional distribution, indicating that the mesochannels in the mesoporous silica thin film have a preferential orientation parallel to the laser induced microgrooves. The degree of orientation calculated from the fwhm of Φ of the two diffraction peaks is as high as 91.8%. Silica MTFs were further prepared on the pattern irradiated PI film with different LIPS depth, and the orientation degree of mesochannels increased with the increase of the LIPS depth as Table S2 (see the Supporting Information).

In-plane XRD measurement was further used to detect the mesochannel orientation distribution along the normal of the silica thin film by changing the incident angle of X-ray. In this measurement, the distribution of mesochannels alignment on the top can be detected by decreasing the angle of incidence X-ray. The orientation degree slightly increased with the increase of incident angle of X-ray, indicating that the orientation

(56) Lu, Q. H.; Wang, Z. G.; Yin, J.; Zhu, Z. K.; Hiraoka, H. *Appl. Phys. Lett*. **2000**, *76*, 1237.
(57) Zhao, Y; Lu, Q. H.; Li, M.; Li, X. *Langmuir* **2007**, *23*, 6212.
(58) Su, B.; Lu, X. M.; Lu, Q. H. *Langmuir* **2008**, *24*, 9695.

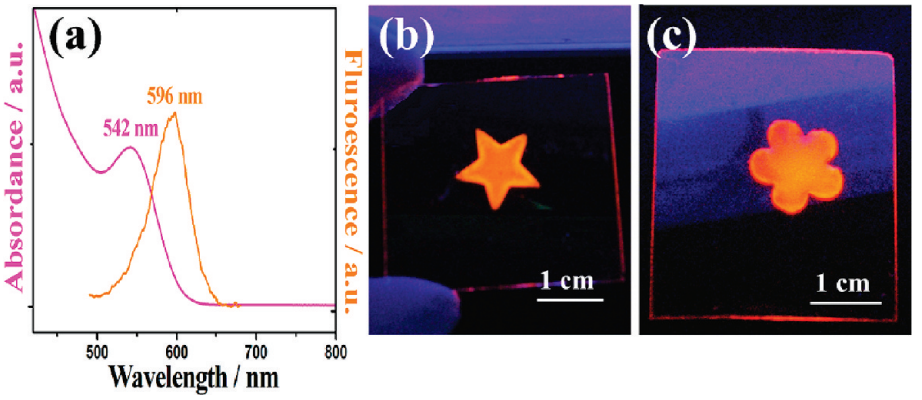

Figure 7. (a) UV−visible absorption spectrum and luminescence spectra of mesoporous silica thin film incorporated with CdTe quantum dots; Optical image of (b) starlike and (c) flower-like mesoporous silica thin film incorporated with CdTe quantum dots. These images were taken under UV lamp irradiation.

distribution of mesochannels was narrower at upper surface than the inner part (Figure S5, see the Supporting Information). However, the deviation of orientation degree is only 1%, indicating that the distribution of mesochannel alignment along the normal direction of oriented mesochannels was nearly uniform on the LIPS surface.

Preparation of the Quantum/Silica Hybrid Film Pattern. The pattern irradiated PI film with LIPS shows strictly controlling ability in on-demand preparation of silica MTFs. The controlling ability comes from the change of the surface properties, including surface topography and wetting property. We also tried to employ above method to prepare patterned quantum dot-incorporated hybrid MTFs, which was widely used in designing a new kind of opto-electro device. The sol precursor solution was mixed with commercial CdTe quantum dots (QD), the diameter of which was about 3−5 nm, corresponding to a UV−vis absorption peak of 542 nm and an emission peak about 596 nm (excitation wavelength was fixed at 542 nm) (shown in Figure 7a) and then prepared hybrid MTFs in the same way as above. Actually, dispersed quantum dots existed both in silica framework[59] and mesopores[60−62] after such incorporation process and hybrid QD/mesostructured films were subsequently formed. Such composited films exhibited high site-selectivity on the laser patterned irradiated PI film as shown in images b and c in Figure 7. In-plane XRD profile proved that the mesochannels in the hybrid thin film was still oriented along the surface microgrooves though the degree of orientation decreases to 77.1% (Figure S6, see the Supporting Information), which was due to the slight deformation of silica wall framework after incorporating QD guests.[63,64] Such a quantum-dot-incorporated mesostructured film was anticipated to have great potential in designing advance nanodevice.

In conclusion, we demonstrated an on-demand pattern of mesoporous silica thin film on PI film using laser beam. The laser-induced difference of surface energy in irradiated and nonirradiated regions resulted into the self-movement of sol solution for perfect site-selective deposition and the confining effect of surface microgrooves in laser irradiated regions leads to the orientation of mesochannels in silica pattern. Lifting speed and line space are the key factors to prepare fine silica pattern. The orientation degree of mesochannels is dependent on the depth of the laser-induced surface microgroove. This method is in effect not only for pure patterned silica mesoporous thin film, but also for that doped with quantum dot molecules. This technique can open a new avenue to employ such oriented mesoporous film as template to incorporate conductive guests and may promisingly satisfy the various need of designing complex microcircuits in many fields.

Acknowledgment. The authors acknowledge the financial supports of the National Science Foundation of China (50902094, 20874059), Shanghai Leading Academic Discipline Project (B202), and "Nano Project" (0652 nm017) of Science and Technology Commission of Shanghai Municipal Government.

Supporting Information Available: Preparation of laser-induced periodic surface structure, change of surface elements before and after laser irradiation, FT-IR spectrum of as-synthesized MTF and ethanol extracted MTF, C1s spectra of PI surface before and after laser irradiation, orientation distribution of mesochannels along film normal, in-plane XRD profile of quantum dot/silica hybrid film, POM image of the mesostructured silica thin film (PDF). This material is available free of charge via the Internet at http://pubs.acs.org.

(59) Gao, F.; Lu, Q. Y.; Zhao, D. Y. *Adv. Mater.* **2003**, *15*, 739.
(60) Gao, F.; Lu, Q. Y.; Zhao, D. Y. *Chem. Phys. Lett.* **2002**, *360*, 585.
(61) Ryu, S. Y.; Bakerski, W.; Lee, T. K.; Hoffmann, M. R. *J. Phys. Chem. C.* **2007**, *111*, 18195.
(62) Zhao, X. G.; Shi, J. L.; Hu, B.; Zhang, L. X.; Hua, Z. L. *J. Mater. Chem.* **2003**, *13*, 399.
(63) Yuan, Z. Y.; Zhou, W.; Zhang, Z. L.; Liu, J. Q.; Wang, J. Z.; Li, H. X.; Peng, L. M. *Surf. Interface Anal.* **2001**, *32*, 193.
(64) Yuan, Z. Y.; Zhou, W.; Su, B. L. *Chem. Phys. Lett.* **2002**, *361*, 307.